



A simple method to estimate actual evapotranspiration from a combination of net radiation, vegetation index, and temperature

Kaicun Wang,¹ Pucui Wang,¹ Zhanqing Li,² M. Cribb,² and Michael Sparrow³

Received 14 December 2006; revised 25 March 2007; accepted 23 May 2007; published 7 August 2007.

[1] Satellite remote sensing is a promising technique for estimating global or regional evapotranspiration (ET). A simple and accurate method is essential when estimating ET using remote sensing data. Such a method is investigated by taking advantage of satellite measurements and the extensive ground-based measurements available at eight enhanced surface facility sites located throughout the Southern Great Plains (SGP) area of the United States from January 2002 to May 2005. Data analysis shows that correlation coefficients between ET and surface net radiation are the highest, followed by temperatures (air temperature or land surface temperature, T_s), and vegetation indices (enhanced vegetation index (EVI) or normalized difference vegetation index (NDVI)). A simple regression equation is proposed to estimate ET using surface net radiation, air or land surface temperatures and vegetation indices. ET can be estimated using daytime-averaged air temperature and EVI with a root mean square error (RMSE) of $\sim 30 \text{ W m}^{-2}$ and a correlation coefficient of 0.91 across all sites and years. ET can also be estimated with comparable accuracy using NDVI and T_s . More importantly, the daytime-averaged ET can also be estimated using only one measurement per day of temperatures (the daytime maximum air temperature or T_s) with comparable accuracy. A sensitivity analysis shows that the proposed method is only slightly sensitive to errors of temperatures, vegetation indices and net surface radiation. An independent validation was made using the measurements collected by the eddy covariance method at six AmeriFlux sites throughout the United States from 2001 to 2006. The land cover associated with the AmeriFlux sites varies from grassland, to cropland and forest. The results show that ET can be reasonably predicted with a correlation coefficient that varies from 0.84 to 0.95 and a bias that varies from 3 W m^{-2} to 15 W m^{-2} and RMSE varying from $\sim 30 \text{ W m}^{-2}$ to $\sim 40 \text{ W m}^{-2}$. The positive bias partly comes from the energy imbalance problem encountered in the eddy covariance method. The proposed method can predict ET under a wide range of soil moisture contents and land cover types.

Citation: Wang, K., P. Wang, Z. Li, M. Cribb, and M. Sparrow (2007), A simple method to estimate actual evapotranspiration from a combination of net radiation, vegetation index, and temperature, *J. Geophys. Res.*, 112, D15107, doi:10.1029/2006JD008351.

1. Introduction

[2] Evapotranspiration (ET) is a primary process driving energy and water exchanges between the hydrosphere, atmosphere and biosphere [e.g., Priestley and Taylor, 1972; Monteith, 1973]. It is required by short-term numerical weather prediction models and longer-term simulations for climate prediction [Rowntree, 1991].

[3] Conventional techniques provide essentially point measurements, which usually do not represent area means because of the heterogeneity of land surfaces and the dynamic nature of heat transfer processes. Satellite remote sensing is a promising tool which has been used to provide reasonable estimates of ET or the evaporative fraction (EF), which is defined as the ratio of ET to available total energy (the difference between surface net radiation and ground heat flux [Shuttleworth *et al.*, 1989]). Over the last few decades a large number of techniques have been proposed to estimate ET (see Drexler *et al.* [2004], Kite and Droogers [2000], Verstraeten *et al.* [2005], and Wang *et al.* [2005d] for review).

[4] Under the assumption that the energy storage of a canopy and energy advection are negligible, ET can be calculated as a residual of the surface net radiation (R_n), the sensible heat flux (H) and ground heat flux (G):

$$ET = R_n - G - H \quad (1)$$

¹Laboratory for Middle Atmosphere and Global Environment Observation, Institute of Atmospheric Physics, Chinese Academy of Sciences, Beijing, China.

²Earth System Science Interdisciplinary Center and Department of Atmospheric and Oceanic Science, University of Maryland, College Park, Maryland, USA.

³International CLIVAR Project Office, National Oceanography Centre, Southampton, UK.

Surface heat flux H is usually determined following the Monin-Oblukhov similarity theory [Monin and Obukhov, 1954] in the following parameterized form [e.g., Friedl, 2002; Drexler et al., 2004; Wang et al., 2005d]:

$$H = \frac{\rho C_p (T_o - T_a)}{r_a} \quad (2)$$

where ρ is the density of air, C_p is the specific heat of air, T_o is the surface aerodynamic temperature, T_a is the near-surface air temperature, and r_a is the aerodynamic resistance. In satellite remote sensing applications, the land surface radiometric temperature (T_s) retrieval is often used instead of the aerodynamic temperature in equation (2) [see, e.g., Kustas et al., 1989].

[5] The methods that use the surface-air temperature gradient require unbiased T_s retrievals and air temperature interpolated from ground-based point measurements. Attempts at estimating spatial variability in air temperature at regional scales with remote sensing suggest an uncertainty of 3–4 K [Goward et al., 1994; Prince et al., 1998]. The uncertainties associated with measurements of the T_s retrievals are on the order of several K [Oku and Ishikawa, 2004; Peres and DaCamara, 2004; Prata and Cechedet, 1999; Sun et al., 2004]. As such, except in areas containing low vegetation cover, this derived surface-air temperature gradient is often comparable to its uncertainties [Caselles et al., 1998; Norman et al., 2000]. Therefore ET estimates are sensitive to land surface temperature or air temperature errors. For example, Timmermans et al. [2007] showed that a ± 3 K error in T_s results in an average error about of 75% of the sensible heat flux for the Surface Energy Balance Algorithm for Land (SEBAL [Bastiaanssen et al., 1998]) and an averaged error of about 45% for the Two Source Energy Balance method (TESE [Norman et al., 1995]) over subhumid grassland and semiarid rangeland.

[6] Two different types of methods have been proposed to reduce the sensitivity of flux retrievals to uncertainties in T_s and air temperature: methods using the temporal variation of T_s [Anderson et al., 1997; Nishida et al., 2003; Norman et al., 2000] and the method using the spatial variation of T_s [e.g., Jiang and Islam, 2001]. The T_s and NDVI spatial variation ($T_s - \text{NDVI}$) method uses spatial information about T_s and NDVI to reduce the requirement of accuracy in the T_s retrievals [Venturini et al., 2004]. Jiang and Islam [2001] estimated EF by interpolating the Priestley-Taylor parameter [Priestley and Taylor, 1972] using the triangular distribution of the $T_s - \text{NDVI}$ spatial variation.

[7] In a previous study, Wang et al. [2006] estimated EF using the day-night T_s difference ($\Delta T_s - \text{NDVI}$) spatial variation method. The method lessens the sensitivity of the EF estimation to the error in the T_s retrievals by using a combination of spatial and temporal T_s and vegetation indices information. However, it is difficult to directly obtain ET from EF because ground heat flux is required, as well as surface net radiation. Nagler et al. [2005a, 2005b] proposed to directly estimate ET over riparian vegetation during the growing season using a simple regression equation that combines Moderate-resolution Imaging Spectroradiometer (MODIS) Enhanced Vegetation Index (EVI) and air temperature. Satellite T_s retrieval were not incorporated into their method because they believe that T_s at 1-km and

5-km resolution is too coarse to characterize temperature over a narrow riparian corridor.

[8] In the present study, advantage is taken of satellite measurements and the extensive ground-based measurements available at the 8 enhanced surface facility sites located throughout the Southern Great Plains (SGP) area of the United States from January 2002 to May 2005. A simple method is proposed based on the data analysis, with input parameters that can be solely obtained from satellite remote sensing data, such as that from MODIS. The sensitivity of the ET estimation to the T_s error greatly decreases and its accuracy is better or comparable to that of the more complicated methods. Independent validation is made using the measurements based upon the eddy covariance method at six AmeriFlux sites throughout the United States from 2001 to 2006.

2. Methodology

2.1. Data and Study Area

[9] Given that satellites can only provide limited information pertaining to ET, a major task in the remote sensing of ET is to identify key factors influencing the processes involved and its parameterization from satellite data. To this end, extensive measurements of surface fluxes, meteorological and soil variables, as well as coincident satellite data are required. This requirement is met thanks to the continuous observations made over the past decade at the SGP sites, such as the Energy Balance Bowen Ratio (EBBR) stations and the Solar and Infrared Radiation Stations (SIRS). Measurements include ET, surface net radiation and its components, related meteorological parameters and soil moisture.

[10] Data collected from eight extended facility sites located throughout the SGP were selected here. Figure 1 shows the International Geosphere-Biosphere Programme (IGBP) land cover types that characterize the study region, and the superimposed locations of the eight enhanced facility sites chosen for this study. Table 1 shows that the eight sites chosen represent a variety of land types, soil moisture and vegetation conditions. Table 1 also shows that these stations are located on uncultivated land such as pastures, grazed and ungrazed rangeland and native prairie. These stations operate continuously throughout the year. The measurements and instruments at the EBBR stations are summarized in Table 2 and SIRS stations measurements and instruments are summarized in Table 3. More details about the SGP sites and the measurements, are given at <http://www.archive.arm.gov/> or by Wang et al. [2006].

[11] SIRS and EBBR data averaged over 30 min were downloaded from <http://www.archive.arm.gov/>, from which daytime-averaged data used in this paper are obtained. The ground data sets cover a period ranging from January 2002 to May 2005.

[12] Coincident satellite data used in this study, such as MODIS land surface products related to ET, including T_s , vegetation indices, albedo, and land cover type were obtained from <http://edcdaac.usgs.gov/modis/dataproduct.html>.

[13] Two MODIS instruments [Salomonson et al., 1989] have been launched for global studies of the atmosphere, land, and ocean processes. The first instrument was launched on 18 December 1999 on a morning platform

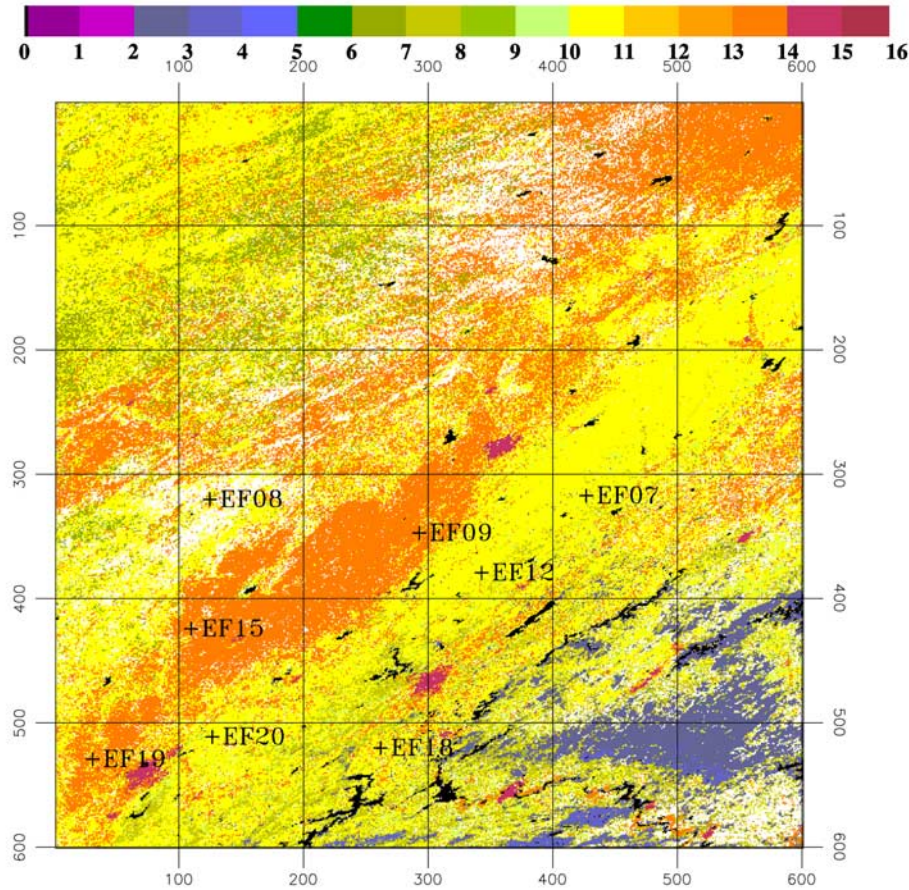


Figure 1. Different land cover types characterizing the Southern Great Plains study region. The pixel resolution is about 1 km and the whole region is about 550 × 550 km². International Geosphere-Biosphere Programme (IGBP) land cover types are shown: 0, water body; 1, evergreen needleleaf forest; 2, evergreen broadleaf forest; 3, deciduous needleleaf forest; 4, deciduous broadleaf forest; 5, mixed forest; 6, closed shrubland; 7, open shrubland; 8, woody savanna; 9, savanna; 10, grassland; 11, permanent wetland; 12, crop land; 13, urban/build up; 14, crop land/natural vegetation mosaic; 15, snow/ice; and 16, barren lands. The locations of the eight enhanced facility (EF) sites are also shown.

called Terra, and the second was launched on 4 May 2002 on an afternoon platform called Aqua. The Terra overpass time is around 1030 (local solar time) in its descending mode and 2230 local solar time in its ascending mode; the

Aqua overpass time is around 1330 local solar time in its ascending mode and 0130 local solar time in its descending mode.

[14] Two algorithms were used to retrieve T_s from the MODIS thermal and middle infrared spectral regions: the

Table 1. Brief Description of the Eight Enhanced Facilities Located Throughout the Southern Great Plains^a

Site	Latitude/Longitude	Elevation, m	Land Cover	Mean (Max) NDVI	Mean (Max) ET	Mean SM
Elk Falls, Kansas: EF07	37.383°N, 96.180°W	283	pasture	0.49 (0.74)	137.9 (256.9)	0.238
Coldwater, Kansas: EF08	37.333°N, 99.309°W	664	rangeland (grazed)	0.36 (0.67)	103.4 (220.2)	0.084
Ashton, Kansas: EF09	37.133°N, 97.266°W	386	pasture	0.49 (0.74)	130.6 (281.4)	0.205
Pawhuska, Oklahoma: EF12	36.841°N, 96.427°W	331	native prairie	0.48 (0.81)	122.4 (305.9)	0.240
Ringwood, Oklahoma: EF15	36.431°N, 98.284°W	418	pasture	0.41 (0.62)	112.3 (261.5)	...
Morris, Oklahoma: EF18	35.687°N, 95.856°W	217	pasture (ungrazed)	0.50 (0.76)	131.0 (248.2)	0.195
El Reno, Oklahoma: EF19	35.557°N, 98.017°W	421	pasture (ungrazed)	0.44 (0.69)	132.4 (307.5)	0.239
Meecker, Oklahoma: EF20	35.564°N, 96.988°W	309	pasture	0.48 (0.70)	128.2 (262.8)	0.205

^aMean and maximum values of NDVI are obtained from the MODIS 16-day vegetation indices product from January 2002 to May 2005. Mean soil moisture (SM, kg/kg) is obtained from surface soil moisture measurements taken at a depth of 2.5 cm, collected from January 2002 to May 2005. Mean evapotranspiration (ET, unit: W m⁻²) are also obtained from data collected from January 2002 to May 2005.

Table 2. Measurements and Instruments Deployed at the Southern Great Plains Energy Balance Bowen Ratio (EBBR) Sites

Measurement	Instrument
Net radiation only	Q*6.1
Ground heat flux	five HFT3.1 ground flux plates installed at 5-cm depth; five REBS PRTDs installed at 0–5 cm depth, spaced 1.0 m apart
Sensible and latent heat fluxes	Bowen ration system; vertical temperature/moisture gradient measured between 2 and 3 m
Soil moisture	five resistance-type SMP-2 sensors, installed at 2.5-cm depth, spaced 1.0 m apart

generalized split window algorithm [Wan and Dozier, 1996] and the MODIS day/night T_s algorithm [Wan and Li, 1997]. Different validations have shown that the MODIS T_s at 1-km resolution produced by the split-window algorithm has an accuracy of ~ 1 K [Coll et al., 2005; Wan et al., 2002, 2004; Wang et al., 2005a, 2007]. The T_s at 1-km resolution has a spatial scale much larger than that of the ground measurements. To keep the scales consistent, the T_s used here is calculated from upwelling longwave radiation (L_u) measurements collected at the SIRS using the Stefan-Boltzmann law:

$$T_s = (L_u / \sigma \varepsilon)^{\frac{1}{4}} \quad (3)$$

where σ is the Stefan-Boltzmann's constant ($5.67 \times 10^{-8} \text{ W m}^{-2} \text{ K}^{-4}$) and ε is the surface broadband emissivity, which can be obtained from MODIS narrowband emissivities in the thermal infrared region from the MODIS day/night T_s products [Wang et al., 2005b].

[15] Two global vegetation index products are available from the MODIS: the NDVI and the EVI [Huete et al., 2002] which are given by:

$$NDVI = (\rho_{nir} - \rho_{red}) / (\rho_{nir} + \rho_{red}) \quad (4)$$

and

$$EVI = 2.6 \times (\rho_{nir} - \rho_{red}) / (\rho_{nir} + 6 \times \rho_{red} + 7.5 \times \rho_{blue} + 1.0) \quad (5)$$

where ρ is reflectance after atmospheric correction, the subscript “nir” represents the MODIS near-infrared band (band 2 at 0.841–0.876 μm), “red” represents the MODIS

red band (band 1 at 0.620–0.670 μm) and “blue” represents the MODIS blue band (band 4 at 0.545–0.565 μm). A 16-day compositing procedure was developed to provide high-quality vegetation index data every 16 days [Van Leeuwen et al., 1999]. The large scale of the MODIS 1-km resolution vegetation data may result in errors in the ET estimation.

2.2. Closely Related Parameters

[16] Data collected from January 2002 to May 2005 are analyzed at the eight sites in order to identify factors that derive the variation of ET.

[17] Figure 2 gives an example of the time series of daytime-averaged ET, air temperature, soil moisture, EVI, and surface net radiation collected at site EF20. Surface net radiation, air temperature, and EVI demonstrate a seasonal variation similar to that of ET. Therefore the correlation coefficients between ET and these parameters are expected to be high. Soil moisture shows a different seasonal variation from that of ET so the correlation coefficients between soil moisture and ET are expected to be low.

[18] Table 4 summarizes the correlation coefficients between ET and the temperatures including near-surface air temperature and T_s , vegetation indices including NDVI and EVI, the surface net radiation and its components, and soil moisture at the eight sites. The daytime-averaged data were used to calculate the correlation coefficients, and the values of daily vegetation indices (NDVI and EVI) are directly obtained from MODIS vegetation indices products, that is to say all daily vegetation indices in the composite period equal to the composite values.

[19] Generally, surface net radiation has the highest correlation coefficient. This is easy to understand because surface net radiation is the energy available to drive surface evaporation and vegetation transpiration [Arora, 2002]. This has been shown by many studies; for example, Priestley and Taylor [1972] demonstrated that the evaporation (or evapotranspiration) over water surfaces and dense vegetation is closely related to the available energy and the evaporation can be solely calculated from the available energy and air temperature using the Priestley-Taylor equation [Wang et al., 2006]. Parlange and Albertson [1995] extended the usage of the Priestley-Taylor equation to general conditions. After comparing 27 models to estimate potential evapotranspiration over a large sample of 308 catchments located in France, Australia and the United States, Oudin et al. [2005] concluded that the surface net radiation and temperature are the most essential controlling parameters for

Table 3. Summary of Solar and Infrared Radiation Station (SIRS) Measurements and Equipment

Measurement	Radiometer Type ^a	Model ^b	Estimated Measurement Uncertainty ^c
Direct normal	pyrheliometer	Normal Incidence Pyrheliometer (NIP)	$\pm 3.0\%$ or 4 W m^{-2}
Diffuse horizontal	pyranometer	Precision Spectral Pyranometer (PSP) (replaced by Model 8–48 (Black and White) after Feb 2000)	$\pm 6.0\%$ or 20 W m^{-2}
Global horizontal	pyranometer	Precision Spectral Pyranometer	$\pm 6.0\%$ or 10 W m^{-2}
Upwelling shortwave	pyranometer	Precision Spectral Pyranometer	$\pm 6.0\%$ or 15 W m^{-2}
Downwelling longwave	pyrgeometer	Precision Infrared Radiometer	$\pm 2.5\%$ or 4 W m^{-2}
Upwelling longwave	pyrgeometer	Precision Infrared Radiometer	$\pm 2.5\%$ or 4 W m^{-2}

^aAll radiometers manufactured by the Eppley Laboratory, Inc., Newport, Rhode Island, USA.

^bShortwave (solar) radiometer spectral responses are 295–3000 nm and longwave (infrared) radiometer spectral responses are 3.5–50 μm .

^cField measurement uncertainties include the uncertainties associated with radiometer calibration and measurement system installation, operation and maintenance. Two standard deviations (95% coverage) were used to account for the random components of the total uncertainty estimates.

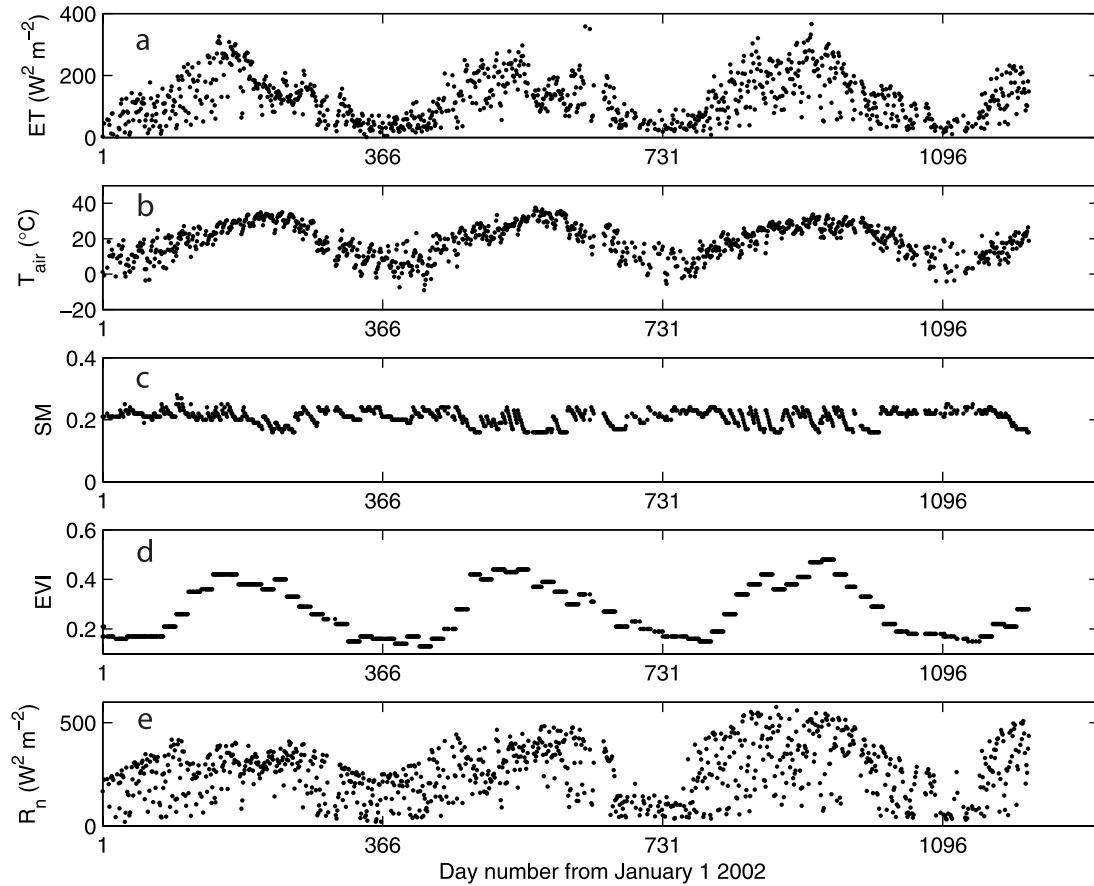


Figure 2. Time series of (a) daytime-averaged evapotranspiration (ET), (b) air temperature (T_{air}), (c) soil moisture (SM), (d) enhanced vegetation index (EVI), and (e) surface net radiation (R_n) collected during January 2002 to May 2005 at site EF20.

estimating potential evapotranspiration. A formula based on surface net radiation and temperature was proposed, which claims to have a better accuracy than those of the more complicated models.

[20] The correlation coefficients between ET and temperatures are the second highest. In addition to daytime-averaged temperatures, daytime maximum values are also used to calculate the correlation coefficients because they are more easily obtained. Daytime maximum air tempera-

ture can be obtained directly from routine weather station observations, and daytime maximum T_s can be obtained from geostationary or polar orbit satellite observations, such as those collected by the Advanced Very High Resolution Radiometer (AVHRR) and MODIS [Aires *et al.*, 2004; Göttsche and Olesen, 2001; Jin and Dickinson, 1999; Jin, 2000]. The correlation coefficients between ET and daytime maximum temperatures are comparable to those between ET and daytime-averaged values, which shows that it is

Table 4. Correlation Coefficients Between Evapotranspiration (ET) and the Daytime-Averaged Air Temperature ($r_{ET,Tad}$), the Daytime Maximum Air Temperature ($r_{ET,Tam}$), Daytime-Averaged Land Surface Temperature ($r_{ET,Tsd}$), Daytime Maximum Land Surface Temperature ($r_{ET,Tsm}$), the Downwelling Shortwave Radiation ($r_{ET,SD}$), the Net Shortwave Radiation ($r_{ET,Sn}$), the Surface Net Radiation ($r_{ET,Rn}$), the Enhanced Vegetation Index (r_{ETEVI}), the Normalized Difference Vegetation Index ($r_{ET,NDVI}$), and Soil Moisture ($r_{ET,SM}$)^a

Site	$r_{ET,Tad}$	$r_{ET,Tam}$	$r_{ET,Tsd}$	$r_{ET,Tsm}$	$r_{ET,SD}$	$r_{ET,Sn}$	$r_{ET,Rn}$	r_{ETEVI}	$r_{ET,NDVI}$	$r_{ET,SM}$
EF07	0.667	0.659	0.676	0.664	0.704	0.747	0.809	0.644	0.624	-0.194
EF08	0.625	0.604	0.622	0.614	0.676	0.710	0.762	0.515	0.409	-0.059
EF09	0.800	0.783	0.832	0.801	0.720	0.749	0.826	0.720	0.664	-0.381
EF12	0.781	0.761	0.769	0.7461	0.683	0.679	0.763	0.800	0.793	-0.5205
EF15	0.708	0.760	0.792	0.778	0.714	0.731	0.788	0.614	0.531	...
EF18	0.745	0.749	0.779	0.782	0.789	0.813	0.864	0.669	0.666	-0.416
EF19	0.687	0.669	0.674	0.663	0.664	0.662	0.736	0.719	0.702	-0.386
EF20	0.682	0.670	0.688	0.682	0.702	0.711	0.773	0.712	0.667	-0.190
Total	0.713	0.700	0.710	0.707	0.695	0.707	0.777	0.680	0.636	-0.101

^aData used here were collected during January 2002 to May 2005. The daily vegetation indices are directly obtained from MODIS 16-day vegetation indices products.

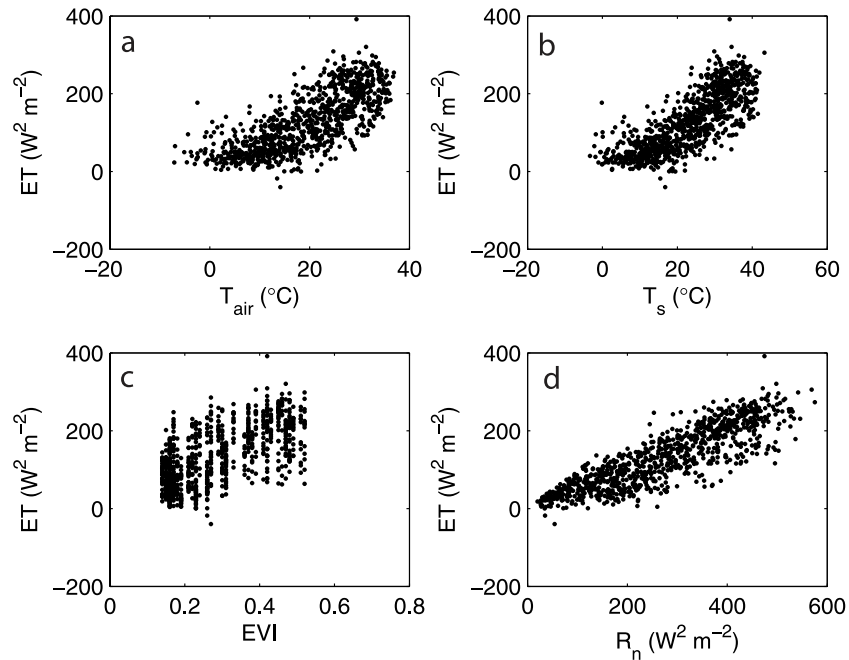


Figure 3. Scatterplots of ET as a function of (a) the daytime-averaged air temperature (T_{air}), (b) daytime-averaged land surface temperature (T_s), (c) enhanced vegetation index (EVI) and (d) surface net radiation (R_n) collected during January 2002 to May 2005 at site EF18.

possible to estimate daytime-averaged ET with only once per day satellite or ground-based measurements.

[21] The vegetation indices are also highly correlated to ET and the correlation coefficients for EVI are a little higher than those for NDVI, which is also found by *Nagler et al.* [2005a, 2005b]. *Suzuki and Masuda* [2004] found that the NDVI is highly correlated to ET at large scales. Vegetation transpiration couples with CO₂ assimilation through the process of vegetation photosynthesis; therefore vegetation amount is one of the determining factors in vegetation transpiration. Vegetation indices along with leaf area index (LAI) have been widely used to quantify the surface vegetation amount [*Tucker, 1979*]. *Arora* [2002] claimed that LAI is the basis of ET parameterizations over vegetation-covered surfaces in physically based hydrological models. Recent studies have shown that ET is closely related to green leaf area and vegetation indices [*Burba and Verma, 2005*; *Li et al., 2006*].

[22] Table 4 also demonstrates that correlation coefficients between soil moisture and ET are low because the seasonal variation differ between soil moisture ET (see also Figure 2). New research shows that when the soil moisture is above the wilting point the influence of soil moisture on ET is very small [*Jaksic et al., 2006*]. This is often the case for vegetation-covered areas. However, soil moisture does influence ET, especially during long drought periods.

2.3. Parameterization of ET

[23] In the above section, it has been shown that surface net radiation, temperatures and vegetation indices are the top three variables correlated with ET. The relationship between ET and these parameters will be further studied in detail in order to accurately parameterize ET.

[24] Figure 3 shows an example of the scatterplots of ET as a function of the daytime-averaged air temperature, the daytime-averaged T_s , the EVI and the surface net radiation collected at site EF18. The relationship between ET and EVI and air temperature are similar to those found by *Nagler et al.* [2005a, Figure 6] and *Nagler et al.* [2005b, Figure 2]. Figure 3 demonstrates that ET increases near linearly with surface net radiation. Therefore it seems reasonable to select surface net radiation as the first factor used to parameterize ET. Global surface radiation estimates of high accuracy have been retrieved from satellite data [e.g., *Allan et al., 2004*; *Bisht et al., 2005*; *Diak et al., 2004*; *Gupta et al., 1999*; *Li and Leighton, 1993*; *Li et al., 2005*; *Wang et al., 2005b, 2005c*; *Zhang et al., 2004*].

[25] Surface net radiation was used to normalize daytime-averaged ET because of their near-linear relationship. Table 5 summarizes the correlation coefficients between the ET normalized by surface net radiation and related parameters. After normalization, vegetation indices have the highest correlation coefficients, and temperatures have the second-highest correlation coefficients. The correlation coefficients between normalized ET and surface net radiation are very low now, which means that the linear relationship is enough to characterize the influence of surface net radiation on ET. The correlation coefficients between soil moisture and normalized ET are still very low, which indicates that the influence of soil moisture on ET is less than that of surface net radiation, vegetation conditions (vegetation indices) and temperatures in vegetated regions.

[26] Figure 4 shows an example of the scatterplots of ET normalized by surface net radiation as a function of the daytime-averaged air temperature, the daytime-averaged T_s , the EVI and the NDVI collected at site EF09. The normalized ET increases near linearly with the two temper-

Table 5. Correlation Coefficients Between the Evapotranspiration (ET_n) Normalized by Surface Net Radiation and the Daytime-Averaged Air Temperature ($r_{ET_n,Tad}$), the Daytime Maximum Air Temperature ($r_{ET_n,Tam}$), Daytime-Averaged Land Surface Temperature ($r_{ET_n,Tsd}$), Daytime Maximum Land Surface Temperature ($r_{ET_n,Tsm}$), the Surface Net Radiation ($r_{ET_n,Rn}$), the Enhanced Vegetation Index ($r_{ET_n,EVI}$), the Normalized Difference Vegetation Index ($r_{ET_n,NDVI}$), and the Soil Moisture ($r_{ET_n,SM}$)^a

Site	$r_{ET_n,Tad}$	$r_{ET_n,Tam}$	$r_{ET_n,Tsd}$	$r_{ET_n,Tsm}$	$r_{ET_n,Rn}$	$r_{ET_n,EVI}$	$r_{ET_n,NDVI}$	$r_{ET_n,SM}$
EF07	0.230	0.191	0.130	0.156	-0.090	0.323	0.316	0.089
EF08	0.117	0.093	-0.008	-0.003	-0.174	0.247	0.247	0.204
EF09	0.460	0.442	0.357	0.273	0.048	0.5187	0.509	-0.127
EF12	0.394	0.359	0.260	0.304	-0.041	0.554	0.569	-0.295
EF15	0.293	0.267	0.151	0.155	-0.142	0.272	0.253	...
EF18	0.308	0.293	0.225	0.250	-0.035	0.359	0.385	-0.117
EF19	0.278	0.233	0.141	0.145	-0.126	0.454	0.461	-0.055
EF20	0.277	0.267	0.193	0.197	-0.039	0.411	0.362	0.027
Total	0.2865	0.258	0.1587	0.179	-0.082	0.415	0.417	0.079

^aData used here were collected during January 2002 to May 2005. The daily vegetation indices are directly obtained from MODIS 16-day vegetation indices products.

atures and vegetation indices. Therefore ET can be parameterized as follows:

$$ET = R_n \cdot (a_0 + a_1 \cdot VI + a_2 \cdot T) \quad (6)$$

where VI can be EVI or NDVI, and T can be daytime-averaged (or daytime maximum) air temperature or T_s . Table 6 summarizes the coefficients used in this parameterization of ET (equation (6)) for different combinations of temperature and vegetation indices using all the daytime-averaged data collected at the 8 sites during January 2002 to May 2005.

2.4. Validity of the Parameterization

[27] Because the vegetation indices data are available on a 16-day basis, we compare the predicted ET with measured ET on a 16-day basis similar to that of Nagler *et al.*

[2005a, 2005b]. It should be noted that the coefficients of equation (6) are obtained using daytime-averaged data (see Table 6), and can be used to predict daytime-averaged ET. Figure 5 shows the time series of the measured and predicted ET using equation (6) with EVI and daytime-averaged air temperature at the 8 sites over the SGP. In general, the measured and predicted seasonal curves are in good agreement.

[28] Table 7 summarizes the statistical parameters of the measured and predicted ET at each site. Figure 6 shows a scatterplot of the measured and predicted ET using equation (6) with EVI and daytime-averaged air temperature at the sites. Table 7 shows that the mean differences between measured and predicted ET are less than 6 W m^{-2} for most sites. The correlation coefficients vary from 0.88 to 0.96 for all 8 sites (Table 6), which are higher than those reported by Nagler *et al.* [2005a, 2005b]. Although the

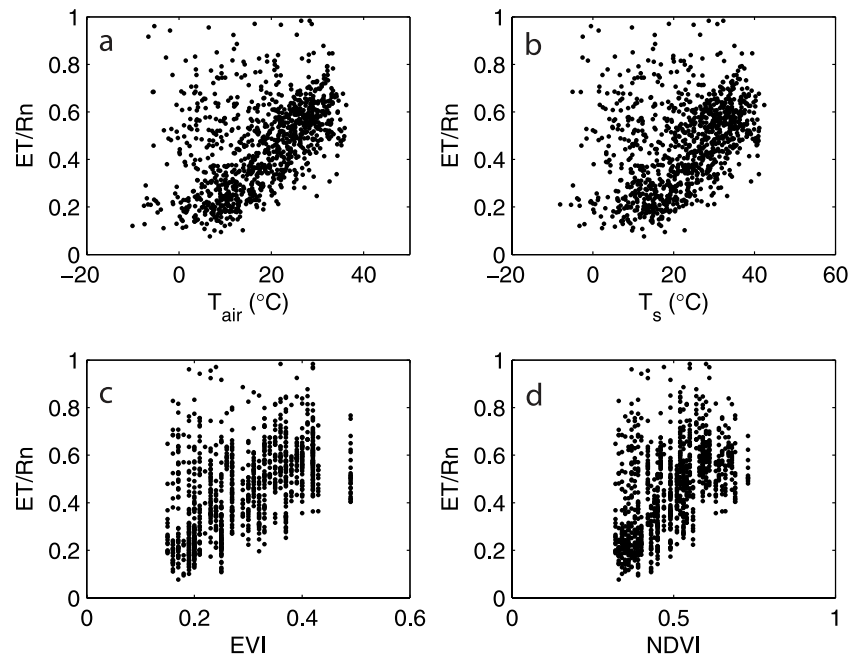


Figure 4. Scatterplots of ET normalized by surface net radiation (ET/R_n) as a function of (a) the daytime-averaged air temperature, (b) the daytime-averaged land surface temperature, (c) the enhanced vegetation index (EVI) and (d) the normalized difference vegetation index (NDVI) collected during January 2002 to May 2005 at site EF09.

Table 6. A Summary of the Regression Coefficients in Equation (6) for Different Combinations of Temperature and Vegetation Index^a

Combination	a_0	a_1	a_2	Correlation Coefficient	RMSE (Relative)	Bias (Relative)
<i>EVI</i> , $T_{a,d}$	0.137	0.759	0.004	0.91	29.2 (24.4%)	1.9 (1.6%)
<i>EVI</i> , $T_{a,m}$	0.114	0.778	0.0039	0.91	29.5 (24.7%)	1.7 (1.4%)
<i>EVI</i> , $T_{s,d}$	0.114	0.778	0.0039	0.91	30.1 (25.2%)	1.7 (1.4%)
<i>EVI</i> , $T_{s,m}$	0.096	0.78	0.0039	0.90	30.4 (25.4%)	1.7 (1.4%)
<i>NDVI</i> , $T_{a,d}$	0.1505	0.45	0.004	0.91	29.2 (24.4%)	-0.7 (-0.5%)
<i>NDVI</i> , $T_{a,m}$	0.106	0.49	0.0039	0.91	29.2 (24.5%)	1.2 (1.0%)
<i>NDVI</i> , $T_{s,d}$	0.106	0.49	0.0039	0.90	29.9 (25.0%)	1.2 (1.0%)
<i>NDVI</i> , $T_{s,m}$	0.084	0.498	0.0039	0.90	30.1 (25.1%)	1.3 (1.1%)

^aThe data collected during January 2002 to May 2005 at the eight sites are used to derive the parameters. The root mean square errors (RMSE) and correlation coefficients between predicted and measured ET are also shown. The relative bias (or RMSE, root mean square error) is the ratio of bias (or RMSE) to the average of measured ET during January 2002 to May 2005. The units for RMSE and Bias are $W m^{-2}$.

correlation coefficients between ET and vegetation indices are less than those reported by Nagler *et al.* [2005a, 2005b], the correlation coefficients between measured and predicted ET in the present study are higher because surface net radiation has been incorporated into the parameterization of ET. The root mean square error (RMSE) of the predicted ET at all sites ranges from $\sim 20 W m^{-2}$ to $\sim 30 W m^{-2}$, with a relative RMSE (ratio to the average of measured ET across all sites and years) of $\sim 20\%$.

[29] Nagler *et al.* [2005a, 2005b] argued that their method should only be used under water unstressed conditions, e.g., for riparian vegetation. At site EF08, soil moisture (at 2.5 cm

is very low, about 0.08 kg/kg (annual average, see Table 1 and Figure 7). However, ET can be predicted with an accuracy comparable to those at sites with high soil water contents. Figure 7 shows that the parameterization can work well for a wide range of soil moisture content. This is similar results found by Jaksic *et al.* [2006], where they showed that when the soil moisture is above the wilting point, the influence of soil moisture on ET is very small. The parameterization will overestimate ET during severe drought conditions, such as during the June–July 2003 period (about day number 510–550) for site EF07 (Figure 7). However, it was found that ET over

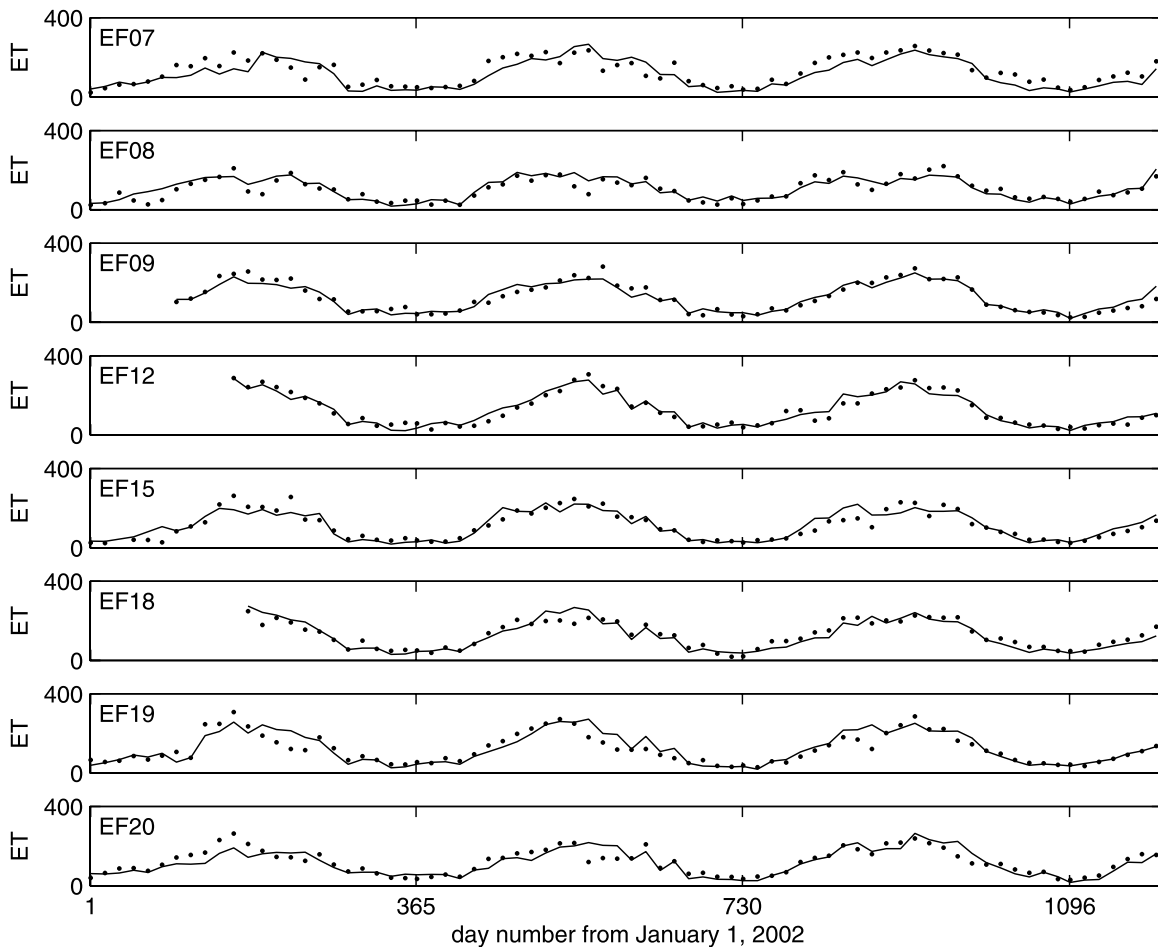


Figure 5. Time series of the measured (dots) and predicted ET (solid lines) using equation (6) with *EVI* and daytime-averaged air temperature at the eight sites.

Table 7. Statistical Parameters of the Measured and Predicted Evapotranspiration (ET) Using Equation (6) With the Enhanced Vegetation Index (EVI) and Daytime-Averaged Air Temperature^a

	EF07	EF08	EF09	EF12	EF15	EF18	EF19	EF20
Correlation coefficient	0.88	0.88	0.95	0.96	0.91	0.94	0.90	0.88
Bias (relative)	-16.1 (-12.4%)	4.5 (4.5%)	-0.7 (-0.5%)	1.1 (0.8%)	2.5 (2.3%)	-5.0 (-3.9%)	4.1 (3.4%)	-5.5 (-4.6%)
RMSE (relative)	33.1 (25.6%)	25.6 (25.3%)	24.0 (19.0%)	22.5 (17.8%)	29.8 (27.4%)	25.8 (20.1%)	34.2 (28.5%)	30.5 (25.6%)

^aRelative bias (or RMSE, root square mean error) is the ratio of bias (or RMSE) to the average of measured ET during January 2002 to May 2005. The units for bias and RMSE are $W\ m^{-2}$.

vegetation is closely related to the root zone soil moisture except in conditions of extreme soil water deficit [Arrett and Clark, 1994; Arora, 2002; Carlson et al., 1994] and therefore depends on different vegetation conditions [Arora, 2002], which complicate the usage of soil moisture content. Given the complication of using soil moisture content, this factor is not incorporated in our current parameterization of ET.

[30] Table 6 demonstrates that NDVI and T_s can also be used to predict ET with comparable accuracy. More importantly, Table 6 demonstrates that the daytime-averaged ET can be predicted with comparable accuracy using once per day temperature measurements, such as daytime maximum air temperature from routine weather observations or daytime maximum T_s from satellite measurements. These data are more easily obtained than 30-min averaged temperature measurements.

2.5. Sensitivity Analysis of the Parameterization

[31] Assuming that interactions between temperature, EVI and net radiation are small enough to be ignored, the sensitivity of ET to temperature (T), EVI and net radiation can be written as:

$$\frac{\partial ET}{\partial T} = R_n \cdot a_2 \tag{7}$$

$$\frac{\partial ET}{\partial EVI} = R_n \cdot a_1 \tag{8}$$

$$\frac{\partial ET}{\partial R_n} = a_0 + a_1 \cdot EVI + a_2 \cdot T \tag{9}$$

Therefore the relative error in ET caused by the errors in temperature, EVI and net radiation (R_n) can be written as:

$$\frac{\Delta ET}{ET} = \frac{\Delta T \cdot a_2}{a_0 + a_1 \cdot EVI + a_2 \cdot T} \tag{10}$$

$$\frac{\Delta ET}{ET} = \frac{\Delta EVI \cdot a_1}{a_0 + a_1 \cdot EVI + a_2 \cdot T} \tag{11}$$

$$\frac{\Delta ET}{ET} = \frac{\Delta R_n}{R_n} \tag{12}$$

For example, if $EVI = 0.35$, $R_n = 350\ W\ m^{-2}$, and $T_{air} = 25^\circ C$, the relative error in ET resulting from an error of $4^\circ C$ in air temperature is 3.8%. The relative error in ET resulting from an error of 0.04 in EVI is 7.8%, and the

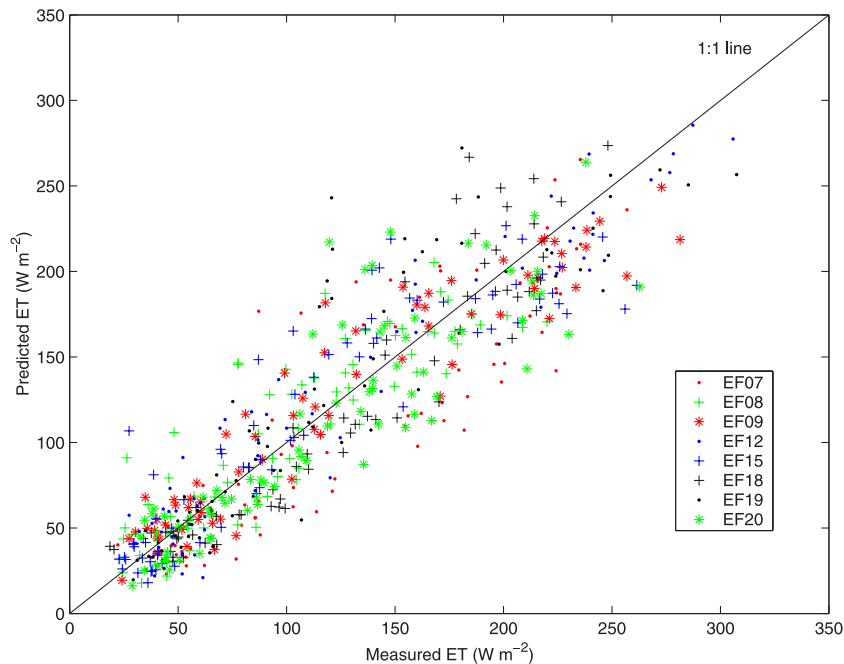


Figure 6. Scatterplot of the predicted ET (using equation (6) with EVI and daytime-averaged air temperature) as a function of the measured ET for the eight sites.

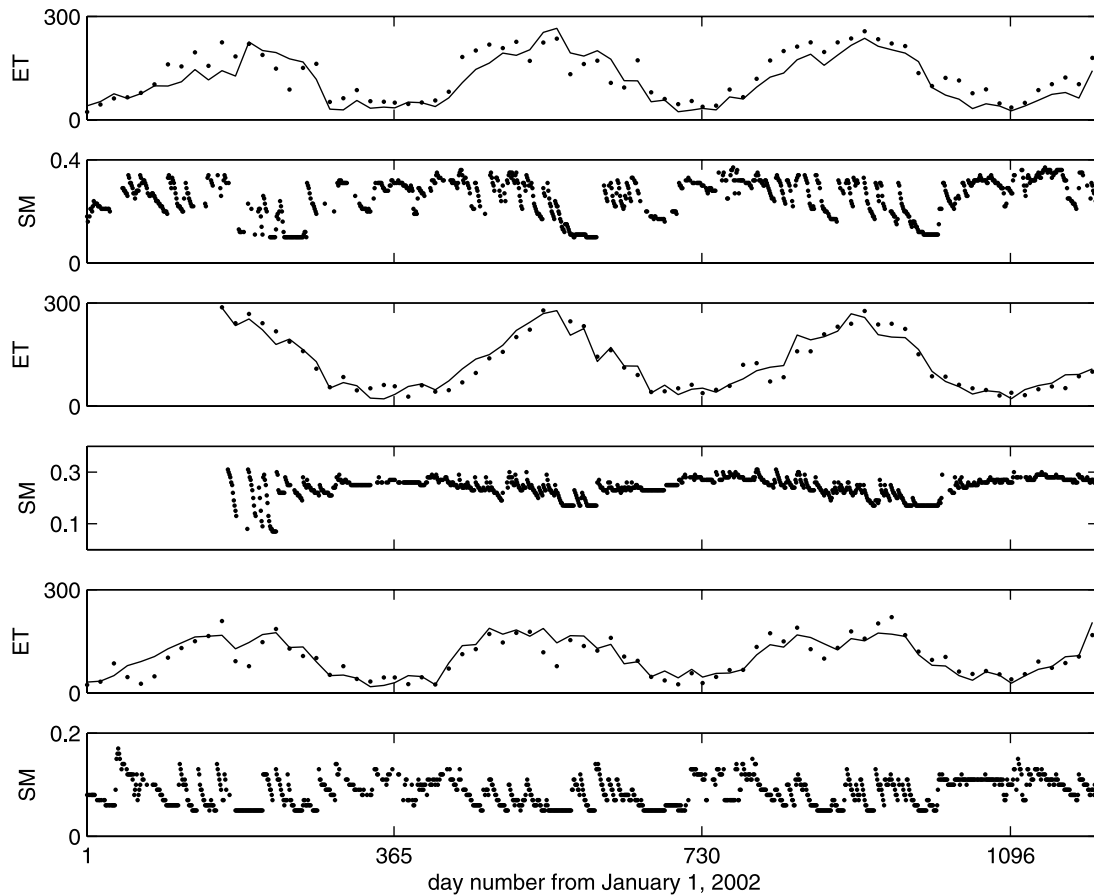


Figure 7. Time series of the measured ET (dots), predicted ET (solid lines) using equation (6) with EVI and daytime-averaged air temperature and soil moisture content (SM, unit: kg/kg, black dots) at three sites.

relative error in ET caused by an error of 20 W m^{-2} in R_n is 5.8%. One can see that the predicted ET is less sensitive to the error in air temperature. The results for other combinations of parameters are similar. The sensitivity is much less than that of methods using surface-air temperature gradients [Timmermans *et al.*, 2007].

3. Independent Validation

[32] It was shown in section 2.4 that ET can be estimated using daytime-averaged air temperature and EVI with a root mean square error (RMSE) of $\sim 30 \text{ W m}^{-2}$, and a correlation coefficient of 0.91 across all sites and years. However, the method needs to be validated by independent data sets. The measurements collected at six AmeriFlux sites ([\[public.ornl.gov/ameriflux/data-get.cfm\]\(http://public.ornl.gov/ameriflux/data-get.cfm\)\) are selected to do so. Table 8 shows a summary of the condition of the AmeriFlux sites located throughout the United States. Compared with the uncultivated land of the SGP sites and the closer geographic proximity of the sites, the land cover types at the AmeriFlux sites vary from grassland, to cropland and forest and their locations are also greatly different from each other.](http://</p>
</div>
<div data-bbox=)

[33] The ET at these AmeriFlux sites is measured by the eddy covariance (EC) method. The eddy covariance method is believed to be the best method to directly measure heat fluxes and is widely used in global measurement experiments, such as FLUXNET (<http://www.daac.ornl.gov/FLUXNET/fluxnet.html>) [Balocchi *et al.*, 2001]. Unfortunately, it suffers from an energy imbalance problem; that is,

Table 8. A Summary of the Conditions at the AmeriFlux Sites Located Throughout the United States^a

Site Name	Land Cover	Latitude	Longitude	Mean (Max) NDVI	Mean (Max) ET	Mean SM	Time Period
Black Hills	evergreen needleleaf forest	44.16	-103.65	0.60 (0.96)	81.3 (262.1)	0.14	2004–2006
Goodwin Creek	temperate grassland	34.25	-89.97	0.61 (0.82)	100.9 (260.9)	0.33	2002–2006
Mead irrigated	irrigated continuous maize-soybean	41.17	-96.48	0.41 (0.92)	88.9 (297.5)	...	2001–2005
Mead irrigated rotation	irrigated maize-soybean rotation	41.18	-96.44	0.43 (0.87)	89.6 (282.5)	...	2001–2005
Mead rainfed	rainfed maize	41.16	-96.47	0.40 (86)	82.3 (252.8)	...	2001–2005
Rayonier	croplands	40.00	-88.29	0.68 (0.90)	81.0 (266.0)	0.33	2001–2005

^aMean and maximum values of NDVI are obtained from MODIS 16-day vegetation indices, and mean soil moisture (SM, kg/kg) is obtained from surface soil moisture measurements taken at a depth of 2.5 cm. Evapotranspiration (ET) has units of W m^{-2} .

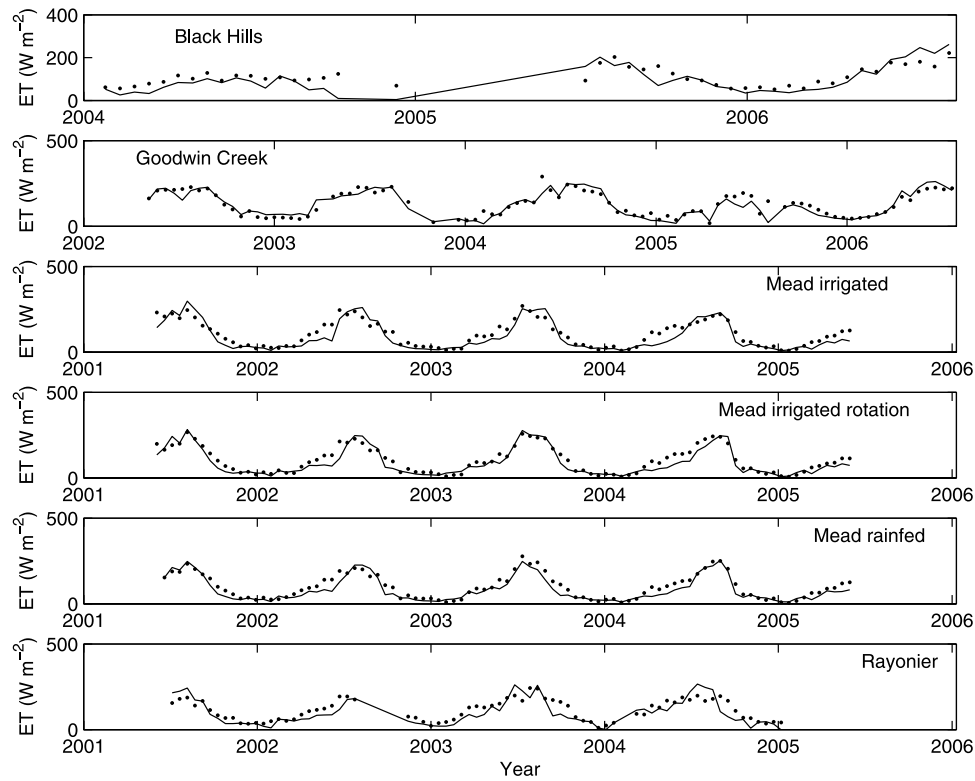


Figure 8. An example of the times series of the measured (solid line) and predicted 16-day average ET (dots) using equation (6) with EVI and daytime-averaged air temperature at the six AmeriFlux sites.

the sum of the measured sensible and latent heat fluxes is not equal to the available energy, which should be equal according to the energy balance law (see equation (1) for an example). The sum is often much less than the available energy, which may result in an underestimation of ET [Wilson et al., 2002]. The method proposed by Twine et al. [2000] is selected to avoid this issue. However, because there are no ground heat flux measurements available at sites Mead Irrigated, Mead Irrigated Rotation and Mead Rainfed, ET at these sites are not corrected.

[34] The parameters in Table 6 obtained from SGP EBBR sites are used to predict ET over the AmeriFlux sites. Figure 8 gives an example of the times series of the measured and predicted 16-day average ET using equation (6) with EVI and daytime-averaged air temperature measured at the six AmeriFlux sites. Table 9 gives the statistical parameters of the measured and predicted 16-day averaged ET using equation (6) with the EVI and daytime-averaged air temperature over the AmeriFlux sites. One can see that the correlation coefficient varies from 0.84 to 0.95, the bias varies from $\sim 3 \text{ W m}^{-2}$ to $\sim 15 \text{ W m}^{-2}$, and the

RMSE varies from $\sim 30 \text{ W m}^{-2}$ to $\sim 40 \text{ W m}^{-2}$. The positive bias may partly come from the energy imbalance issue of the eddy covariance method because the EC method can underestimate ET and no correction is carried out at sites of Mead Irrigated, Mead Irrigated Rotation and Mead Rainfed because of data limited. The other combinations of vegetation indices and temperature give similar results (not shown).

[35] Jiang and Islam [2001] reported an RMSE of 85.3 W m^{-2} (29% of the mean ET) by using the linear NDVI-LST spatial variation method with NOAA-AVHRR data and an interpolated surface net radiation map over the SGP area for 2001. Batra et al. [2006] showed that ET can be estimated with a RMSE of 53, 51 and 56.24 W m^{-2} , and a correlation coefficient of 0.84, 0.79 and 0.77 from MODIS, NOAA16 and NOAA14 sensors respectively. Nishida et al. [2003] reported that the bias, RMSE and correlation coefficients for ET were 5.59 W m^{-2} , 45.06 W m^{-2} and 0.86, respectively, from a comparison of NOAA-AVHRR data with data from AmeriFlux stations spread over the continental United States. Norman et al. [2003] reported that the

Table 9. Statistical Parameters of the Measured and Predicted 16-Day Average Evapotranspiration (ET) Using Equation (6) With the Enhanced Vegetation Index (EVI) and Daytime-Averaged Air Temperature Over the AmeriFlux Sites Listed in Table 8^a

	Black Hills	Goodwin Creek	Mead Irrigated	Mead Irrigated Rotation	Mead Rainfed	Rayonier
Correlation coefficient	0.84	0.92	0.92	0.94	0.95	0.85
Bias, W m^{-2}	13.9	3.4	14.2	12.4	15.0	14.1
RMSE, W m^{-2}	36.5	29.3	33.4	27.4	23.8	38.7

^aThe parameters obtained from the data generated by the Energy Balance Bowen Ration (EBBR) method collected over the Southern Great Plains (Table 6).

ET estimated by combining low (GOES) and high (aircraft) resolution (~ 24 m) remote sensing data had a RMSE of about 40 W m^{-2} . The ET estimated from more complicated models also demonstrates comparable uncertainties [e.g., *Rivas and Caselles, 2004*].

[36] The required ET retrieval accuracy varies according to application, but is typically 50 W m^{-2} , as suggested by *Seguin et al. [1999]*. The accuracy of this study meets this requirement. At the same times, *Jiang et al. [2004]* also show that a reasonable upper limit to the accuracy of remote sensing methods for obtaining ET is about 20%.

4. Conclusions

[37] A simple and accurate method is essential to estimate ET using remote sensing data. The suitability of the method also depends on the practicability of the required input data. In the present study, this was done by taking advantage of satellite measurements and the extensive ground-based measurements available at 8 enhanced surface facility sites located throughout the Southern Great Plains from January 2002 to May 2005.

[38] The dominant factors driving the seasonal variation of ET are surface net radiation, temperatures and vegetation indices. Correlation coefficients between surface net radiation and ET are the highest, followed by temperatures and vegetation indices. A simple regression equation is obtained to estimate ET using surface net radiation, air or land surface temperatures and vegetation indices.

[39] ET predicted from the equation using a combination of surface net radiation, daytime-averaged air temperature and enhanced vegetation index (EVI) has an average RMSE of $\sim 30 \text{ W m}^{-2}$, and the correlation coefficients between measured and predicted ET vary from 0.88 to 0.96 for all the sites. ET can also be estimated from NDVI and T_s with comparable accuracy. More importantly, daytime-averaged ET can be estimated using only one measurement of temperature (daytime maximum air temperature or T_s) per day with comparable accuracy. The daytime maximum air temperature can be obtained directly from routine observations made at weather stations, and T_s can be derived from geostationary or polar orbit satellite observations. Sensitivity analysis shows that the proposed method is less sensitive to the errors in temperature, vegetation indices and net radiation than that of the method using surface-air temperature gradient.

[40] Independent validation is carried out using the measurements from eddy covariance method at six AmeriFlux sites located throughout the United States from 2001 to 2006. The land cover of the sites varies from grassland, to cropland and forest. The results show that ET can be predicted with correlation coefficients that vary from 0.84 to 0.95, biases that vary from $\sim 3 \text{ W m}^{-2}$ to $\sim 15 \text{ W m}^{-2}$, and RMSE varying from $\sim 30 \text{ W m}^{-2}$ to $\sim 40 \text{ W m}^{-2}$. The positive bias may partly come from the energy imbalance issue encountered in the eddy covariance method.

[41] *Arora [2002]* argued that photosynthesis and transpirational water losses are strongly linked, and therefore the net primary production and evapotranspiration from vegetation are coupled. *Nemani et al. [2003]* believed that temperature, surface radiation and water are the three most important climate factors influencing net primary produc-

tion and they further showed that the influence of radiation and temperature are much larger than that of water in the present study region. Development of the proposed method shows a similar conclusion. The results reported by *Nemani et al. [2003]* also suggest that the simple equation proposed here may be suitable on a wide basis. However, more data and studies are needed to investigate its suitability for other areas and cover types. The method proposed here should be confined to regions where surface net radiation is a major controlling factor of ET [*Nemani et al., 2003*] and should be used with caution in areas where energy advection is important.

[42] Soil moisture content is not incorporated into the parameterization of ET introduced here. *Jaksic et al. [2006]* argue that when the soil moisture is above the wilting point its influence on ET is very small. The equation can predict ET under a wide range of soil moisture contents and land covers. However, the parameterization will overestimate ET during severe drought conditions.

[43] The input data of the proposed method, e.g., surface net radiation, temperature and vegetation indices, can be solely obtained from satellite measurements. Given the input parameters, regional ET distributions are easily generated.

[44] **Acknowledgments.** We would like to thank the anonymous reviewers for their critical and helpful comments and suggestions. This research was jointly funded by the U.S. Department of Energy's Atmospheric Radiation Program with grant DEFG0201ER63166, the National Science Foundation of China (40520120071) and an opening funding of the National Key Laboratory for Remote Sensing Science (SK050012).

References

- Aires, F., C. Prigent, and W. Rossow (2004), Temporal interpolation of global surface skin temperature diurnal cycle over land under clear and cloudy conditions, *J. Geophys. Res.*, *109*, D04313, doi:10.1029/2003JD003527.
- Allan, R. P., M. A. Ringer, J. A. Pamment, and A. Slingo (2004), Simulation of the Earth's radiation budget by the European Centre for Medium-Range Weather Forecasts 40-year reanalysis (ERA40), *J. Geophys. Res.*, *109*, D18107, doi:10.1029/2004JD004816.
- Anderson, M. C., J. M. Norman, G. R. Diak, W. P. Kustas, and J. R. Mecikalski (1997), A two-source time-integrated model for estimating surface flux using thermal infrared remote sensing, *Remote Sens. Environ.*, *60*, 195–216.
- Arora, V. (2002), Modeling vegetation as a dynamic component in soil-vegetation-atmosphere transfer schemes and hydrological models, *Rev. Geophys.*, *40*(2), 1006, doi:10.1029/2001RG000103.
- Arrett, R. W., and C. A. Clark (1994), Functional relationship among soil moisture, vegetation cover and surface fluxes, in *Proceedings 21st Conference in Agricultural and Forest Meteorology*, Abstr. J37-J38, Am. Meteorol. Soc., San Diego, Calif., 7–11 March.
- Baldocchi, D., et al. (2001), FLUXNET: A new tool to study the temporal and spatial variability of ecosystem-scale carbon dioxide, water vapor and energy flux densities, *Bull. Am. Meteorol. Soc.*, *82*, 2415–2434.
- Bastiaanssen, W. G. M., M. Menenti, R. A. Feddes, and A. A. M. Holtslag (1998), A remote sensing surface energy balance algorithm for land (SEBAL): 1. Formulation, *J. Hydrol.*, *212*(1), 198–212.
- Batra, N., S. Islam, V. Venturini, G. Bisht, and L. Jiang (2006), Estimation and comparison of evapotranspiration from MODIS and AVHRR sensors for clear sky days over the southern Great Plains, *Remote Sens. Environ.*, *103*, 1–15.
- Bisht, G., V. Venturini, S. Islam, and L. Jiang (2005), Estimation of the net radiation using MODIS (Moderate Resolution Imaging Spectroradiometer) data for clear sky days, *Remote Sens. Environ.*, *97*, 52–67.
- Burba, G. G., and S. B. Verma (2005), Seasonal and interannual variability in evapotranspiration of native tallgrass prairie and cultivated wheat ecosystems, *Agric. For. Meteorol.*, *135*, 190–201.
- Carlson, T. N., R. R. Gillies, and E. M. Perry (1994), A method to make use of thermal infrared temperature and NDVI measurements to infer surface soil water content and fractional vegetation cover, *Remote Sens. Rev.*, *9*, 161–173.

- Caselles, V., M. M. Artigao, E. Hurtado, C. Coll, and A. Brasa (1998), Mapping actual evapotranspiration by combining landsat TM and NOAA-AVHRR images: Application to the Barrax area, Spain, *Remote Sens. Environ.*, *63*, 1–10.
- Coll, C., V. Caselles, J. M. Galve, E. Valor, R. Niclos, J. M. Sanchez, and R. Rivas (2005), Ground measurements for the validation of land surface temperatures derived from AATSR and MODIS data, *Remote Sens. Environ.*, *97*, 288–300.
- Diak, G. R., J. R. Mecikalski, M. C. Anderson, J. M. Norman, W. P. Kustas, R. D. Torn, and R. L. DeWolf (2004), Estimating land surface energy budgets from space: Review and current efforts at the University of Wisconsin-Madison and USDA-ARS, *Bull. Am. Meteorol. Soc.*, *85*(1), 65–78.
- Drexler, J., R. Snyder, D. Spano, K. Ta, and U. Paw (2004), A review of models and micrometeorological methods used to estimate wetland evapotranspiration, *Hydrol. Processes*, *18*, 2071–2101.
- Friedl, M. A. (2002), Forward and inverse modeling of land surface energy balance using surface temperature measurements, *Remote Sens. Environ.*, *79*, 344–354.
- Göttsche, F. M., and F. K. Olesen (2001), Modelling of diurnal cycles of brightness temperature extracted from METEOSAT data, *Remote Sens. Environ.*, *76*, 337–348.
- Goward, S. N., R. H. Waring, D. G. Dye, and J. Yang (1994), Ecological remote sensing at OTTER: Satellite macroscale observations, *Ecol. Appl.*, *4*, 322–343.
- Gupta, S. K., N. A. Ritchey, A. C. Wilber, C. H. Whitlock, G. G. Gibson, and P. W. Stackhouse Jr. (1999), A climatology of surface radiation budget derived from satellite data, *J. Clim.*, *12*, 2691–2710.
- Huete, A., K. Didan, T. Miura, E. P. Rodriguez, X. Gao, and L. G. Ferreira (2002), Overview of the radiometric and biophysical performance of the MODIS vegetation indices, *Remote Sens. Environ.*, *83*, 195–213.
- Jaksic, V., G. Kiely, J. Albertson, R. Oren, G. Katul, P. Leahy, and K. A. Byrne (2006), Net ecosystem exchange of grassland in contrasting wet and dry years, *Agric. For. Meteorol.*, *139*, 323–334.
- Jiang, L., and S. Islam (2001), Estimation of surface evaporation map over southern Great Plains using remote sensing data, *Water Resour. Res.*, *37*(2), 329–340.
- Jiang, H., et al. (2004), The influence of vegetation type on the hydrological process at the landscape scale, *Can. J. Remote Sens.*, *30*(5), 743–763.
- Jin, M. (2000), Interpolation of surface radiation temperature measured from polar orbiting satellites to a diurnal cycle: Part 2. Cloudy-pixel treatment, *J. Geophys. Res.*, *105*(D3), 4061–4076.
- Jin, M., and R. E. Dickinson (1999), Interpolation of surface radiation temperature measured from polar orbiting satellites to a diurnal cycle: Part 1. Without clouds, *J. Geophys. Res.*, *104*, 2105–2116.
- Kite, G. W., and P. Droogers (2000), Comparing evapotranspiration estimates from satellite hydrological models and field data, *J. Hydrol.*, *229*, 3–18.
- Kustas, W., B. Choudhury, M. M. R. Reginato, R. Jackson, L. Gay, and H. Weaver (1989), Determination of sensible heat flux over sparse canopy using thermal infrared data, *Agric. For. Meteorol.*, *44*, 197–216.
- Li, S.-G., W. Eugster, J. Asanuma, A. Kotani, G. Davaa, D. Oyunbaatar, and M. Sugita (2006), Energy partitioning and its biophysical controls above a grazing steppe in central Mongolia, *Agric. For. Meteorol.*, *137*, 89–106.
- Li, Z., and H. G. Leighton (1993), Global climatologies of solar radiation budgets at the surface and in the atmosphere from 5 years of ERBE data, *J. Geophys. Res.*, *98*, 4919–4930.
- Li, Z., M. Cribb, F.-L. Chang, A. Trishchenko, and L. Yi (2005), Natural variability and sampling errors in solar radiation measurements for model validation over the ARM/SGP Region, *J. Geophys. Res.*, *110*, D15S19, doi:10.1029/2004JD005028.
- Monin, A. S., and A. M. Obukhov (1954), Basic laws of turbulent mixing in the atmosphere near the ground. *Trudy Geofizicheskogo Instituta Akademiyi Nauk SSSR*, *24*(151), 163–187.
- Monteith, J. L. (1973), *Principles of Environmental Physics*, 241 pp., Edward Arnold, London.
- Nagler, P. L., J. Cleverly, E. Glenn, D. Lampkin, A. Huete, and Z. Wan (2005a), Predicting riparian evapotranspiration from MODIS vegetation indices and meteorological data, *Remote Sens. Environ.*, *94*(1), 17–30.
- Nagler, P. L., R. L. Scott, C. Westenburg, J. R. Cleverly, E. P. Glenn, and A. R. Huete (2005b), Evapotranspiration on western US rivers estimated using the enhanced vegetation indices from MODIS and data from eddy covariance and Bowen ratio flux towers, *Remote Sens. Environ.*, *97*(3), 337–351.
- Nemani, R. R., C. D. Keeling, H. Hashimoto, W. M. Jolly, S. C. Piper, C. J. Tucker, R. B. Myneni, and S. W. Running (2003), Climate driven increases in global terrestrial net primary production from 1982–1999, *Science*, *300*, 1560–1563.
- Nishida, K., R. R. Nemani, S. W. Running, and J. M. Glassy (2003), An operational remote sensing algorithm of land surface evaporation, *J. Geophys. Res.*, *108*(D9), 4270, doi:10.1029/2002JD002062.
- Norman, J. M., W. P. Kustas, and K. S. Humes (1995), A two-source approach for estimating soil and vegetation energy fluxes in observations of directional radiometric surface temperature, *Agric. For. Meteorol.*, *77*, 263–293.
- Norman, J. M., W. P. Kustas, J. H. Prueger, and G. R. Diak (2000), Surface flux estimation using radiometric temperature: A dual temperature-difference method to minimize measurement errors, *Water Resour. Res.*, *36*(8), 2263–2274.
- Norman, J. M., M. C. Anderson, W. P. Kustas, A. N. French, J. Mecikalski, R. Torn, G. R. Diak, T. J. Schmugge, and B. C. W. Tanner (2003), Remote sensing of surface energy fluxes at 10¹-m pixel resolutions, *Water Resour. Res.*, *39*(8), 1221, doi:10.1029/2002WR001775.
- Oku, Y., and H. Ishikawa (2004), Estimation of land surface temperature over the Tibetan Plateau using GMS data, *J. Appl. Meteorol.*, *43*, 548–561.
- Oudin, L., F. Hervieu, C. Mickel, C. Perrin, V. Andréassian, F. Anctil, and C. Loumagne (2005), Which potential evapotranspiration input for a lumped rainfall-runoff model? Part 2—Towards a simple and efficient potential evapotranspiration model for rainfall-runoff modeling, *J. Hydrol.*, *303*, 290–306.
- Parlange, M. B., and J. D. Albertson (1995), Regional scale evaporation and the atmospheric boundary layer, *Rev. Geophys.*, *33*(1), 99–124.
- Peres, L. F., and C. C. DaCamara (2004), Land surface temperature and emissivity estimation based on the two-temperature method: Sensitivity analysis using simulated MSG/SEVIRI data, *Remote Sens. Environ.*, *91*, 377–389.
- Prata, A. J., and R. P. Cechet (1999), An assessment of the accuracy of land surface temperature determination from the GMS-5 VISSR, *Remote Sens. Environ.*, *67*, 1–14.
- Priestley, C. H. B., and R. J. Taylor (1972), On the assessment of surface heat flux and evaporation using large-scale parameters, *Mon. Weather Rev.*, *100*, 81–92.
- Prince, S. D., S. J. Goetz, R. O. Dubayah, K. P. Czajkowski, and M. Thawley (1998), Inference of surface and air temperature, atmospheric precipitable water and vapor pressure deficit using advanced very high-resolution radiometer satellite observations: Comparison with field observations, *J. Hydrol.*, *212*(1), 230–249.
- Rivas, R., and V. Caselles (2004), A simplified equation to estimate spatial reference evaporation from remote sensing-based surface temperature and local meteorological data, *Remote Sens. Environ.*, *93*, 68–76.
- Rowntree, P. R. (1991), Atmospheric parameterization for evaporation over land: Basic concept and climate modeling aspects, in *Land Surface Evaporation Fluxes: Their Measurements and Parameterization*, edited by T. J. Schmugge and J. C. André, pp. 5–30, Springer, New York.
- Salomonson, V., W. Barnes, P. Maymon, H. Montgomery, and H. Ostrow (1989), MODIS: Advanced facility instrument for studies of the Earth as a system, *IEEE Trans. Geosci. Remote Sens.*, *27*, 145–153.
- Seguin, B., et al. (1999), IRSUTE: A mini-satellite project for land surface heat flux estimation from field to regional scale, *Remote Sens. Environ.*, *68*, 357–369.
- Shuttleworth, W. J., R. J. Gurney, A. Y. Hsu, and J. P. Ormsby (1989), FIFE: The variation in energy partition at surface flux sites, in *Remote Sensing and Large-Scale Processes*, edited by A. Rango, Proc. of the IAHS Third International Assembly, Baltimore, Md., *IAHS Publ.*, *186*, 67–74.
- Sun, D., R. T. Pinker, and J. B. Basara (2004), Land surface temperature estimation from the next generation of Geostationary Operational Environmental Satellites: GOES M–Q, *J. Appl. Meteorol.*, *43*, 363–372.
- Suzuki, R., and K. Masuda (2004), Interannual co-variability found in evapotranspiration and satellite-derived vegetation indices over northern Asia, *J. Meteorol. Soc. Jpn.*, *82*(4), 1233–1241.
- Timmermans, W. J., W. P. Kustas, M. C. Anderson, and A. N. French (2007), An intercomparison of the Surface Energy Balance Algorithm for Land (SEBAL) and Two-Source Energy Balance (TSEB) modeling Schemes, *Remote Sens. Environ.*, *108*(4), 369–384.
- Tucker, C. J. (1979), Red and photographic infrared linear combinations for monitoring, *Remote Sens. Environ.*, *8*, 127–150.
- Twine, T., et al. (2000), Correcting eddy-covariance flux underestimates over a grassland, *Agric. For. Meteorol.*, *103*, 279–300.
- Van Leeuwen, W., A. Huete, and T. Laing (1999), MODIS vegetation index compositing approach: A prototype with AVHRR data, *Remote Sens. Environ.*, *69*, 264–280.
- Venturini, V., G. Bisht, S. Islam, and L. Jiang (2004), Comparison of EFs estimated from AVHRR and MODIS sensors over south Florida, *Remote Sens. Environ.*, *93*, 77–86.
- Verstraeten, W. W., F. Veroustraete, and J. Feyen (2005), Estimating evapotranspiration of European forests from NOAA-imagery at satellite over-

- pass time: Towards an operational processing chain for integrated optical and thermal sensor data products, *Remote Sens. Environ.*, *96*, 256–276.
- Wan, Z., and J. Dozier (1996), A generalized split-window algorithm for retrieving land-surface temperature from space, *IEEE Trans. Geosci. Remote Sens.*, *34*(4), 892–905.
- Wan, Z., and Z.-L. Li (1997), A physics-based algorithm for retrieving land-surface emissivity and temperature from EOS/MODIS data, *IEEE Trans. Geosci. Remote Sens.*, *35*(4), 980–996.
- Wan, Z., Y.-L. Zhang, Q.-C. Zhang, and Z.-L. Li (2002), Validation of the land surface temperature products retrieved from terra moderate resolution imaging spectroradiometer data, *Remote Sens. Environ.*, *83*, 163–180.
- Wan, Z., Y.-L. Zhang, Q.-C. Zhang, and Z.-L. Li (2004), Quality assessment and validation of the MODIS global land surface temperature, *Int. J. Remote Sens.*, *25*(1), 261–274.
- Wang, K., J. Liu, Z. Wan, P. Wang, M. Sparrow, and S. Haginoya (2005a), Preliminary accuracy assessment of MODIS land surface temperature products at a semi-desert site, *Proc. SPIE Int. Soc. Opt. Eng.*, *5832*, 452–460.
- Wang, K., Z. Wan, P. Wang, M. Sparrow, J. Liu, X. Zhou, and S. Haginoya (2005b), Estimation of surface long wave radiation and broadband emissivity using Moderate Resolution Imaging Spectroradiometer (MODIS) land surface temperature/emissivity products, *J. Geophys. Res.*, *110*, D11109, doi:10.1029/2004JD005566.
- Wang, K., X. Zhou, J. Liu, and M. Sparrow (2005c), Estimating surface solar radiation over complex terrain using moderate-resolution satellite sensor data, *Int. J. Remote Sens.*, *26*(1), 47–58.
- Wang, K., X. Zhou, W. Li, J. Liu, and P. Wang (2005d), Using satellite remotely sensed data to retrieve sensible and latent heat fluxes: A review, (in Chinese with English abstract), *Adv. Geosci.*, *20*(1), 42–48.
- Wang, K., Z. Li, and M. Cribb (2006), Estimation of evaporative fraction from a combination of day and night land surface temperature and NDVI: A new method to determine the Priestley–Taylor parameter, *Remote Sens. Environ.*, *102*, 293–305.
- Wang, K., Z. Wan, P. Wang, M. Sparrow, J. Liu, and S. Haginoya (2007), Evaluation and improvement of the MODIS land surface temperature/emissivity products using ground-based measurements at a semi-desert site on the western Tibetan Plateau, *Int. J. Remote Sens.*, *28*(11), 2549–2565.
- Wilson, K., et al. (2002), Energy balance closure at FLUXNET sites, *Agric. For. Meteorol.*, *113*, 223–243.
- Zhang, Y., W. B. Rossow, A. A. Lacis, V. Oinas, and M. I. Mishchenko (2004), Calculation of radiative fluxes from the surface to top of atmosphere based on ISCCP and other global data sets: Refinements of the radiative transfer model and the input data, *J. Geophys. Res.*, *109*, D19105, doi:10.1029/2003JD004457.

M. Cribb and Z. Li, Earth System Science Interdisciplinary Center and Department of Atmospheric and Oceanic Science, University of Maryland, College Park, MD 20742, USA.

M. Sparrow, International CLIVAR Project Office, National Oceanography Centre, Southampton SO14 3ZH, UK.

K. Wang and P. Wang, Laboratory for Middle Atmosphere and Global Environment Observation, Institute of Atmospheric Physics, Chinese Academy of Sciences, Beijing 100029, China. (wangkaicun@mail.iap.ac.cn)